

# DFA-NeRF: Personalized Talking Head Generation via Disentangled Face Attributes Neural Rendering

Shunyu Yao RuiZhe Zhong Yichao Yan Guangtao Zhai Xiaokang Yang

Shanghai Jiao Tong University

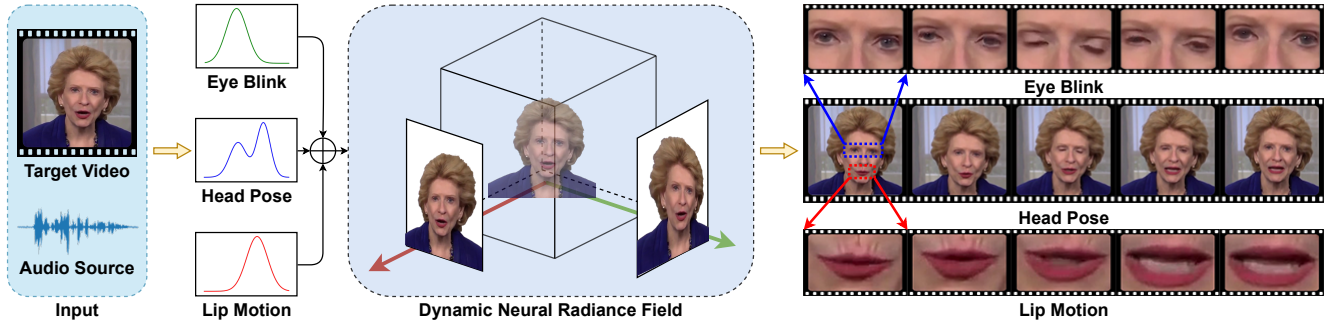


Figure 1. Illustration of Disentangled Face Attributes Neural Radiance Field (DFA-NeRF). Our framework disentangles the face attributes into head poses, eye blink features and lip motion features, which are generated from the input audio. Then we train a dynamic NeRF conditioned on these features to synthesize high-quality personalized talking head images.

## Abstract

While recent advances in deep neural networks have made it possible to render high-quality images, generating photo-realistic and personalized talking head remains challenging. With given audio, the key to tackling this task is synchronizing lip movement and simultaneously generating personalized attributes like head movement and eye blink. In this work, we observe that the input audio is highly correlated to lip motion while less correlated to other personalized attributes (e.g., head movements). Inspired by this, we propose a novel framework based on neural radiance field to pursue high-fidelity and personalized talking head generation. Specifically, neural radiance field takes lip movements features and personalized attributes as two disentangled conditions, where lip movements are directly predicted from the audio inputs to achieve lip-synchronized generation. In the meanwhile, personalized attributes are sampled from a probabilistic model, where we design a Transformer-based variational autoencoder sampled from Gaussian Process to learn plausible and natural-looking head pose and eye blink. Experiments on several benchmarks demonstrate that our method achieves significantly better results than state-of-the-art methods.

## 1. Introduction

Synthesizing dynamic talking head driven by audio is of great importance to various applications, such as film production and online meeting. However, generating photo-realistic and expressive talking heads remains an open challenge, which not only contain accurate lip motions, but also present personalized eye blinks and head movements.

Traditional talking head generation models [49, 9, 47, 42, 60, 12] focus on synthesizing audio-synchronized lip motion, but only generate lip motion with fixed head poses. To address this issue, some recent works consider personalized attributes [52, 55, 58, 50, 48, 7]. However, these methods [52, 55, 58] generate personalized information with a deterministic model and the results are short of diversity, leading to a repetitive pattern. Most of works utilize Generative Adversarial Networks (GAN) [7, 9] to generate the final images. However, GAN is prone to fall into mode collapse and it can only generate images with a fixed resolution. Recently, Neural Radiance Field (NeRF) [31] achieves to render high-quality talking head images with unlimited resolution [21, 19, 29]. Nevertheless, these works neglect the personalized face attributes and fail to synchronize audio with lip motion accurately.

In this work, we propose a novel framework, which we name Disentangled Face Attributes Neural Radiance Field

(DFA-NeRF), to capture synchronized lip motion and personalized attributes simultaneously. As shown in Fig. 1, instead of directly feeding the audio into neural radiance field [21], we propose first to predict the lip motion and personalized attributes from audio and then optimize dynamic NeRF conditioning on these features to synthesize talking head images. In this way, lip motion and personalized attributes are regarded as two disentangled representations, which guarantees the generated images to be lip-synchronized and have natural movement.

The remaining question is how to predict these two types of features from audios. Our critical insight is that lip motion is highly related to auditory phonetics, while the personalized information, such as head poses and eye blinks, is weakly associated with audio and varies from person to person. Therefore, we argue that the key to tackling this challenge lies in two folds. **1)** As audio is strongly correlated with lip motion, it is more appropriate to approximate the lip motion with a deterministic model. Inspired by the recent success of contrastive learning in audio-visual synchronization tasks [56, 32], we introduce a contrastive learning strategy to synchronize the audio feature with the feature of lip motion. **2)** The personalized attributes such as head poses and eye blinks are random and probabilistic. In order to model the distribution of the attributes and generate long time series, we propose a probabilistic model named Transformer Variational Autoencoder (VAE). VAE [5] can generate smooth output and map the data into Gaussian distribution, while the attention mechanism in Transformer [44] helps VAE learn the long-time dependence for time series. Furthermore, we model the temporal dynamics in the Transformer-VAE with a Gaussian Process (GP). With the deterministic and probabilistic model, our framework can generate disentangled motion features that align well with the talking head, providing better conditions for neural rendering.

In summary, our contributions include **1)** We propose two disentangled conditions (*i.e.*, lip motion and personalized attributes) for neural radiance field to generate high-fidelity and natural talking head. **2)** We propose a self-supervised learning method based on AutoEncoder to disentangle lip motion and personalized attributes. **3)** We design a deterministic model to synchronize audio and lip motion and a probabilistic model to generate personalized attributes. **4)** We conduct extensive experiments on several benchmarks, and results demonstrate our method outperforms the state-of-the-art methods in generating high-quality talking head.

## 2. Related Work

**Audio-Driven Talking Head Generation.** Generating photo-realistic video portraits in line with any input audio stream has long been a popular research topic in com-

puter graphics and vision [16, 17, 6]. Some methods aim at finding out the exact correspondence between audio and frames [39, 11, 56, 27, 59, 15, 34, 38, 40].

However, these methods usually ignore head motion since it is hard to separate head posture from facial movement. Some methods are based on the 3D face reconstruction algorithm [20, 2, 46, 14, 12] and GAN [13, 35, 52, 28]. They estimate intermediate representations such as 3D face shapes [24, 43, 52] or 2D landmarks [53, 45] to assist the generation process. Unfortunately, low-dimensional intermediate representation is not capable of describing dynamic face deformations. Unlike these methods, instead of directly using intermediate face representations, our method only extracts the 3DMM face expression parameters to disentangle the mouth features and eye blink features in an implicit way. Moreover, the disentangled mouth features will synchronize with audio features in a high-dimensional latent space. Recently, the neural radiance field (NeRF) [31, 36, 41, 25] has been widely applied in 3D-related tasks because it can accurately reproduce complex scenes with implicit neural representation. Some recent works *et al.* [21, 19] leverage NeRF to represent faces with audio features as conditions. Zhou *et al.* [57] modularizes audio-visual representations by devising an implicit low-dimension pose code.

Our framework is also built on NeRF. Instead of directly sending the audio to NeRF, we propose two disentangled representations to provide improved conditions.

**Personalized Face Attributes Generation.** Personalized attributes are essential for generating natural talking head and have been studied in several prior methods. Yi *et al.* [52] use LSTM [22] to process the input audio to generate expression and head pose. However, the generated head poses are predicted with a deterministic model, lacking diversity. MakeItTalk [37] generates head pose through LSTM and MLP. However, for the LSTM network, the generation process is an auto-regressive task, making the head pose tend to *freeze*. In FACIAL [54], GAN is applied to learn attributes of the given audio and video, whereas the generation process is not explainable nor controllable. LSP [30] adopts a multi-dimensional Gaussian distribution to model the probabilistic process of head poses and body motions. The problem is that the distribution must be learned from scratch for different targets.

We propose a Transformer GP-VAE to generate personalized attributes, such as head poses and eye blinks. The Transformer architecture enables the model to generate long time series, and the VAE makes the generation process controllable and explainable. Furthermore, to model the temporal dynamics of the face attributes sequences, we adopt Gaussian Process to sample in VAE’s latent space. The main differences between other methods and our approach are summarized in Table 1.

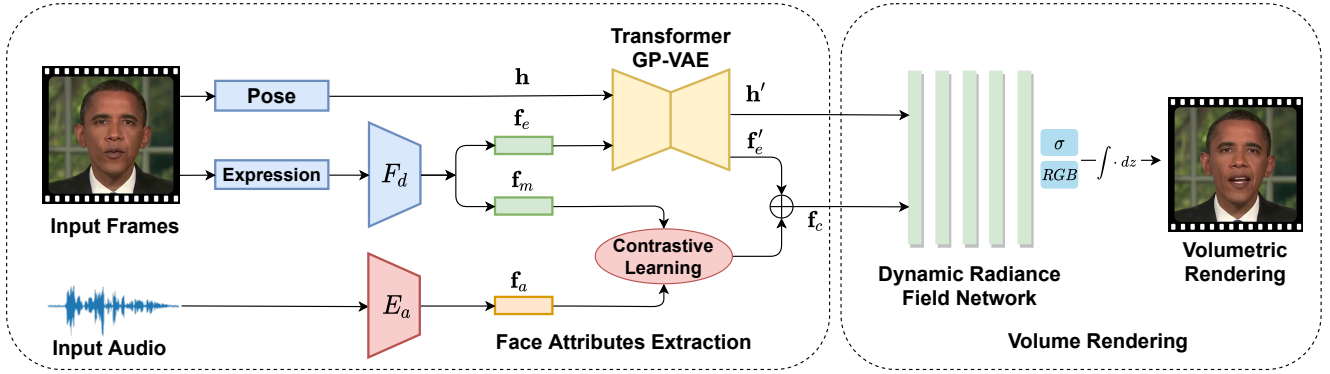


Figure 2. An overview of our proposed framework. Our method mainly consists of two parts: face attributes extraction and volume rendering. For the first part, pose and expression parameters are extracted from input videos. Then face attributes disentanglement module  $F_d$  is introduced to disentangle eye blink embeddings  $\mathbf{f}_e$  and lip motion embeddings  $\mathbf{f}_m$ . We use Transformer GP-VAE to generate personalized attributes such as head poses and eye blink features. We use a contrastive learning method for the lip motion to synchronize the audio feature  $\mathbf{f}_a$  with the mouth movement feature  $\mathbf{f}_m$ . Afterward, in the volume rendering stage, we use generated pose  $\mathbf{h}'$  as the view direction. Meanwhile, the generated eye blink feature and synchronized audio feature are concatenated and serve as a condition  $\mathbf{f}_c$  of the NeRF. Finally, we use volume rendering to render the image.

Aspects	ATVG[9]	Wav2lip[34]	MakeItTalk[58]	LSP[30]	Yi <i>et al.</i> [52]	Chen <i>et al.</i> [7]	FACIAL[54]	AD-NeRF[21]	Ours
Target	arbitrary	arbitrary	arbitrary	specific	specific	arbitrary	arbitrary	specific	specific
Audio feature	not sync	sync	not sync	not sync	not sync	not sync	not sync	not sync	sync
Framework	GAN	GAN	GAN	GAN	GAN	GAN	GAN	NeRF	NeRF
Personalized	No	No	heads, eyes	heads, eyes	heads, eyes	heads	heads, eyes	No	heads, eyes
Face models	2D landmarks	No	2D landmarks	2D landmarks	3DMM	3DMM	3DMM	No	No

Table 1. We conclude five different aspects of several talking head generation works compared to our method: the methods work for a specific target or arbitrary images; The audio feature is synchronized with lip motions or not; The network architecture for image synthesis; The ability to generate personalized attributes and if they use any intermediate face models.

### 3. Approach

#### 3.1. Overview

As shown in Fig. 2, given a source speech audio, our framework aims to construct natural talking heads. First, we extract the pose and 3DMM face expression parameters from video frames. We then design an AutoEncoder  $F_d$  to disentangle the expression parameters into eye blink embeddings  $\mathbf{f}_e$  and mouth embeddings  $\mathbf{f}_m$  in a self-supervised manner. In the meantime, the input audio is sent to a CNN model to extract the audio features  $\mathbf{f}_a$ . After that, we design a contrastive learning method to get the synchronized audio feature  $\mathbf{f}_c$ . For head pose  $\mathbf{h}$  and eye blink embeddings  $\mathbf{f}_e$ , a Transformer VAE with Gaussian Process is designed to model the probabilistic characteristic of these attributes. Finally, a dynamic NeRF is introduced to generate the final image with these conditions.

#### 3.2. Face Attributes Disentanglement

We use 3D Morphable Face Models (3DMM) [33] to extract face expression parameters. The 3D face landmark

coordinates  $\mathbf{S}$  can be represented as the combination of 3DMM expression and geometry parameters:

$$\mathbf{S} = \bar{\mathbf{S}} + \mathbf{B}_{id}\mathbf{F}_{id} + \mathbf{B}_{exp}\mathbf{F}_{exp}, \quad (1)$$

where  $\bar{\mathbf{S}} \in \mathbb{R}^{3N}$  is the averaged facial mesh,  $\mathbf{B}_{id}$  and  $\mathbf{B}_{exp}$  are the PCA basis of geometry and expression.  $\mathbf{F}_{id}$  and  $\mathbf{F}_{exp}$  are the coefficients of geometry and expression basis. Then we select 68 points in the facial mesh  $\mathbf{S}$  to get the face landmarks  $\mathbf{l}$  as in FaceWarehouse [4].

Whereas the expression code of 3DMM is entangled and unexplainable because it is based on PCA, which makes it difficult to control the movement of the mouth and eyes separately. In order to generate disentangled face attributes, we propose a self-supervised learning method strategy. Specifically, we design a fully connected AutoEncoder, as shown in Fig. 3.  $\mathbf{l}_{m_A}^{e_A}$  denotes the face landmarks of a target A. The subscript  $m_A$  means the mouth landmarks of target A and  $e_A$  denotes the eye landmarks. The AutoEncoder generates two intermediate embeddings  $\mathbf{f}_m$ ,  $\mathbf{f}_e$  with an encoder, which can be represented as  $\mathbf{f}_{m_A}, \mathbf{f}_{e_A} = E_L(\mathbf{l}_{m_A}^{e_A})$ . In the meantime, the decoder can be represented as  $\mathbf{l}_{m_A}^{e_A} =$

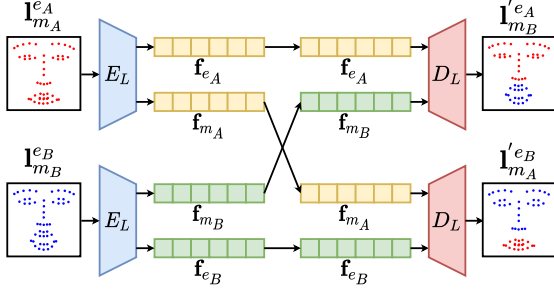


Figure 3. Illustration of face attributes disentanglement: the mouth embedding code is switched as an example.  $\mathbf{f}_e$  represents the eye blink embedding code,  $\mathbf{f}_m$  denotes the mouth embedding code. The subscripts  $A$  and  $B$  indicate different people.

$D_L(\mathbf{f}_{m_A}, \mathbf{f}_{e_A})$ , which will be utilized to reconstruct the face landmarks with  $L_1$  loss. Given another face  $B$  and the corresponding face landmark  $\mathbf{l}_{m_B}^{e_B}$ , we randomly switch the mouth embedding  $\mathbf{f}_m$  or eye blink embedding  $\mathbf{f}_e$  with their corresponding landmarks of face  $A$  and  $B$ . Afterwards, we can reconstruct different landmarks with:

$$\mathcal{L}_{rec} = \|\mathbf{l}_{m_B}^{e_A} - \mathbf{l}_{m_B}^{e_A}\|_1 + \|\mathbf{l}_{m_A}^{e_B} - \mathbf{l}_{m_A}^{e_B}\|_1. \quad (2)$$

In this way, the AutoEncoder can reconstruct the face landmarks with different combinations of face attributes. Consequently, the embedding  $\mathbf{f}_e$  and  $\mathbf{f}_m$  can represent eyes and mouth movement in the learned latent space.

### 3.3. Audio-Lip Synchronization

After obtaining the mouth embedding  $\mathbf{f}_m$ , we need to establish the relationship between the lip motion and the input audio. As indicated by previous works [34, 56], learning the natural synchronization between visual mouth movements and auditory utterances is valuable for the talking face generation. Instead of using visual clues, we choose to synchronize the mouth movement embedding with the auditory utterances directly. Specifically, we employ a CNN audio encoder  $E_a$  to extract the phonemic feature  $\mathbf{f}_a$  from the input audio:  $\mathbf{f}_a = E_a(\mathbf{a})$ , where  $\mathbf{a}$  denotes the input audio data. We adopt a contrastive learning strategy to align audio features with mouth features to seek their synchronization. Specifically, we regard the timely aligned audio and mouth features  $(\mathbf{f}_a, \mathbf{f}_m)$  as a positive pair, while the non-aligned pair  $(\mathbf{f}_a^-, \mathbf{f}_m)$  is treated as negative.

We use the binary cross-entropy loss for contrastive learning, where the distance between timely aligned audio-mouth pairs should be closer than non-aligned pairs:

$$\mathcal{L}_{con} = -\frac{1}{N} \sum_{i=1}^N y_i \log(d(\mathbf{f}_m, \mathbf{f}_a)) + (1 - y_i) \log(1 - d(\mathbf{f}_m, \mathbf{f}_a^-)), \quad (3)$$

where  $d(\mathbf{f}_a, \mathbf{f}_m) = \frac{\mathbf{f}_a \cdot \mathbf{f}_m}{\|\mathbf{f}_a\|_2 \cdot \|\mathbf{f}_m\|_2}$  denotes the cosine distance,  $y_i = 1$  for positive samples and  $y_i = 0$  for negative sam-

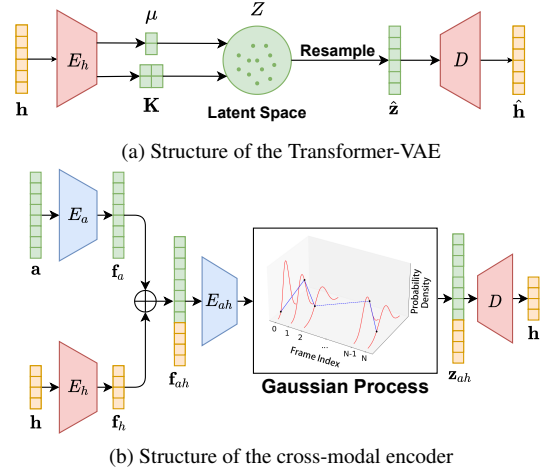


Figure 4. a) Structure of Transformer VAE. This module will structure the input face attribute sequences  $\mathbf{h}$  and learn a Gaussian prior latent space  $Z$ . The encoder  $E_h$  and decoder  $D$  are both Transformers. b) Structure of Transformer-based cross-modal encoder. Audio and BOP sequences share a common feature space, same as the trained latent space  $Z$  in (a). We use the reparameterization trick to resample new latent codes  $\mathbf{z}_{ah}$  through Gaussian Process. The trained decoder  $D$  decodes  $\mathbf{z}_{ah}$  to predict future face attributes.

ples and the total number of samples is  $N$ . During training, we randomly sample timely aligned audio and mouth sequences as positive pairs, while the negative pairs come from different videos or the same video with a time-shift.

### 3.4. Personalized Attributes Generation

To generate personalized attributes such as eye blinks and head poses, we propose a controllable probabilistic model named Transformer GP-VAE in Fig. 4, aiming to generate smooth and long time series. Given a face attribute (head poses or eye blinks) sequence  $\mathbf{h}_{1:T}$  with length  $T$  and a more extended conditioning audio sequence  $\mathbf{a}_{1:T'}$  with length  $T'$ , we need to generate the face attribute embeddings  $\mathbf{h}_{T+1:T'}$  of the future  $T' - T$  frames. Our method consists of two major parts. (1) Latent space construction, where we train a Transformer-VAE with Gaussian Process (GP) on a large dataset to build a mapping between the input face attributes sequence and a latent space  $Z$ . (2) Face attributes generation, where we fine-tune a cross-modal encoder on a selected person to embed both Beginning of Pose (BOP) and audio into the learned latent space  $Z$ . Thus, we can generate new face attributes sequences in an autoregressive manner. Different from the original GP-VAE [18] and MGP-VAE [3], our Transformer GP-VAE can generate various-length time series with cross-modal input.

**Latent Space Construction.** Assume our dataset contains  $N$  continuous time series  $\mathbf{h}^{(i)} \in \mathbb{R}^{T \times d}$ , where  $T$  is the

length of sequence and  $d$  is the dimension of the vector. We construct VAE with a Transformer illustrated in Fig. 4a. We have also considered LSTM, but its outputs tend to converge to a fixed value and have no variations. The multi-head attention mechanism and fully-connected attention in Transformer tackle this frame-freezing problem. The detailed comparison experiments will be discussed in Section 4.

Specifically, the VAE aims to map the time series  $\mathbf{h}$  to a multivariate normal distribution (latent space  $Z$ ) with mean vector  $\boldsymbol{\mu}$  and covariance matrix  $\mathbf{K}$ :

$$\boldsymbol{\mu} = \boldsymbol{\mu}_\phi(\mathbf{h}), \mathbf{K} = \mathbf{K}_\phi(\mathbf{h}), \quad (4)$$

where  $\phi$  are parameters of the encoder  $E_h$  in VAE and the posterior distribution of  $\mathbf{z} \in Z$  is presented as:

$$q_\phi(\mathbf{z} | \mathbf{h}) = \mathcal{N}(\boldsymbol{\mu}, \mathbf{K}). \quad (5)$$

Then we use the reparameterization trick to resample  $\hat{\mathbf{z}} \sim q_\phi(\mathbf{z} | \mathbf{h})$  and decode it into  $\hat{\mathbf{h}} = D(\hat{\mathbf{z}})$ . The Mean Square Error (MSE) with batch size  $B$  is calculated to reconstruct  $\hat{\mathbf{h}}$ :

$$\mathcal{L}_{rec} = \frac{1}{B} \sum_{i=1}^B \|\hat{\mathbf{h}}^{(i)} - \mathbf{h}^{(i)}\|_2. \quad (6)$$

Considering the prior distribution of  $\mathbf{z} \in Z$ , the data points should be  $N$  i.i.d. samples in the original VAE [26]. A time sequence does not satisfy such property due to the solid temporal correlation among frames. To address this, we utilize Gaussian Process to model the temporal correlation. Given the time indices  $\mathbf{t}$  and the corresponding  $\mathbf{z}$  in  $Z$  space, the prior distribution of  $\mathbf{z}$  is:

$$p(\mathbf{z}) = \mathcal{N}(\boldsymbol{\mu}(\mathbf{t}), \mathbf{K}(\mathbf{t}, \mathbf{t})), \quad (7)$$

where  $\boldsymbol{\mu}(\mathbf{t})$  and  $\mathbf{K}(\mathbf{t}, \mathbf{t})$  are determined by the kernel function in GP, which we employ Cauchy kernel function [18]. KL divergence is calculated between prior and posterior distributions as another loss term:

$$\mathcal{L}_{KL} = \text{KL}(p(\mathbf{z}), q_\phi(\mathbf{z} | \mathbf{h})). \quad (8)$$

After the VAE is trained, we can get the distribution of  $\mathbf{z}$  and the corresponding latent space  $Z$ . As we train the VAE with a large dataset, the model can generalize well because the latent space  $Z$  contains different face attributes of the training sequences.

**Face Attributes Generation.** We fine-tune a cross-modal encoder on a selected person to generate personalized face attributes illustrated in Fig. 4b. To generate novel face attributes, we need to encode both audio and BOP of a selected person into the trained latent space  $Z$  in VAE, where audio serves as the conditional information and BOP is needed for initialization. Besides, the trained encoder  $E_h$  and decoder  $D$  in VAE will be used in this stage.

For the audio information, we employ the same audio encoder  $E_a$  which has been used in the audio-lip synchronization module to extract the input audio feature  $\mathbf{f}_a = E_a(\mathbf{a}_{1:T})$ . In the meantime, we use the trained encoder ( $E_h$ ) in Transformer VAE to encode the BOP to the trained latent space  $Z$ , i.e.,  $\mathbf{f}_h = E_h(\mathbf{h}_{1:\tau})$ , where  $\tau$  is the length of BOP sequence. Afterwards, these two features are concatenated in temporal dimension as  $\mathbf{f}_{ah} = [\mathbf{f}_a : \mathbf{f}_h]$  and fed into  $E_{ah}$  to get the mean vector  $\boldsymbol{\mu}'$  and covariance matrix  $\mathbf{K}'$  of cross-modal latent codes  $\mathbf{z}$ 's distribution like  $\mathbf{z} \sim \mathcal{N}(\boldsymbol{\mu}', \mathbf{K}')$ . We use the reparameterization trick to resample  $\mathbf{z}_{ah}$  from  $\mathcal{N}(\boldsymbol{\mu}', \mathbf{K}')$  with Gaussian Process. Finally, the trained decoder ( $D$ ) in Transformer VAE will decode  $\mathbf{z}_{ah}$  into the predicted time series  $\hat{\mathbf{h}}_{\tau+1:T} = D(\mathbf{z}_{ah})$ . The loss function of training cross-modal encoder can be calculated as:

$$\mathcal{L}_{CME} = \frac{1}{B} \sum_{i=1}^B \left\| \hat{\mathbf{h}}_{\tau+1:T}^{(i)} - \mathbf{h}_{\tau+1:T}^{(i)} \right\|. \quad (9)$$

In the test phase, we feed the given audio and BOP to the cross-modal encoder to get the distribution of  $\mathbf{z}_{ah}$ . By resampling  $\mathbf{z}_{ah}$  in this distribution and feeding  $\mathbf{z}_{ah}$  to decoder  $D$ , we can get the generated future face attributes. Note that we can also sample  $\mathbf{z}$  in the trained latent space  $Z$  and feed it to the decoder to generate various face attributes without the input audio, which makes our Transformer-VAE more universal and controllable.

### 3.5. Neural Scene Representation for Talking Head

After obtaining the generated head poses, eye blink features  $\mathbf{f}_e$  and synchronized audio features  $\mathbf{f}_a$ , we employ a neural radiance field to generate the final image with these conditions. We first concatenate audio embedding  $\mathbf{f}_a$  and eye blink embedding  $\mathbf{f}_e$  into a new embedding  $\mathbf{f}_c$ . Then we present a conditional radiance field with this new embedding serving as input. After we transform the head pose from camera space into canonical space, we can directly use the head pose to replace the view direction  $\mathbf{d}$  of the radiance field. Finally, the embedding  $\mathbf{f}_c$ , view direction  $\mathbf{d}$  and 3D location  $\mathbf{x}$  in canonical space constitute the input of the implicit function  $F_\theta$ . In practice,  $F_\theta$  is realized by a multi-layer perceptron. With all concatenated input vectors, the network  $F_\theta$  will estimate color values  $\mathbf{c}$  accompanied with densities  $\sigma$  along with the dispatched rays. The entire implicit function can be formulated as:

$$F_\theta : (\mathbf{f}, \mathbf{d}, \mathbf{x}) \longrightarrow (\mathbf{c}, \sigma). \quad (10)$$

Then we can employ the volume rendering process by accumulating the sampled density  $\sigma$  and RGB values  $\mathbf{c}$  along with the rays  $r$  cast through each pixel to compute the output color  $C(\mathbf{r})$  for image rendering results. Finally, we use

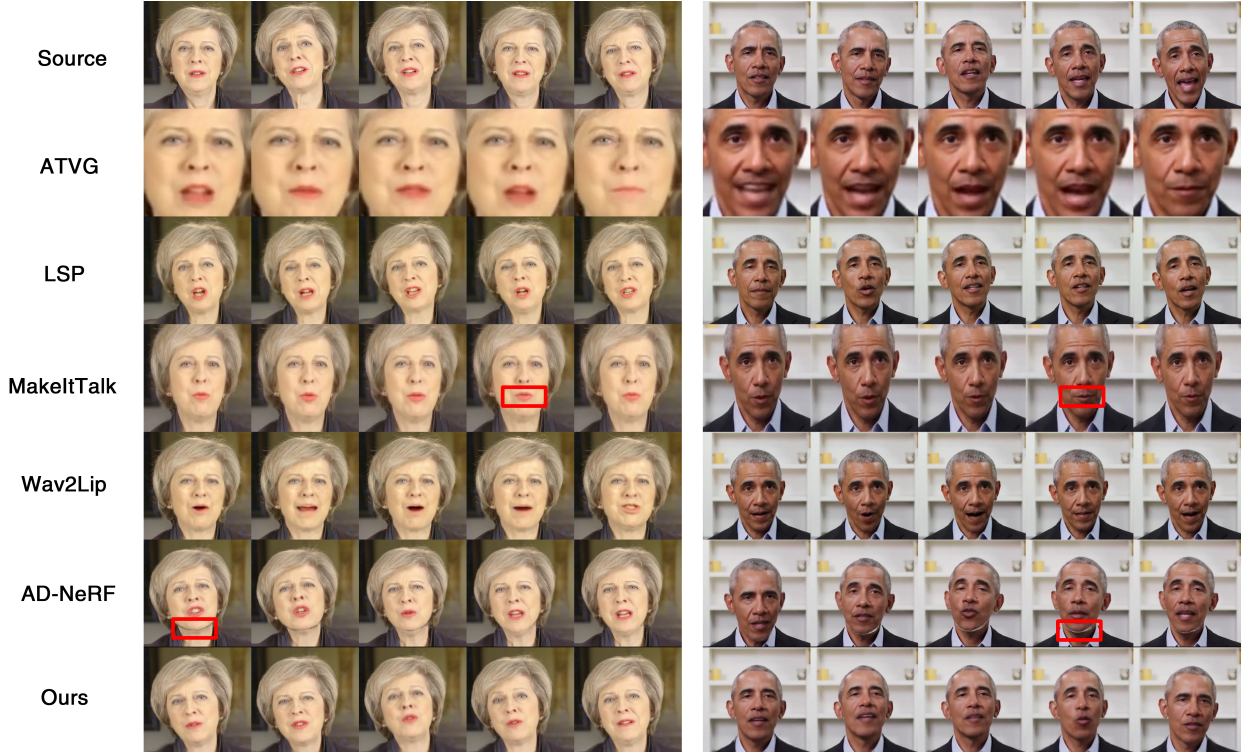


Figure 5. Qualitative results. The top rows are the reference source videos. ATVG [9] can only generate the cropped frontal talking head. LSP [30] can generate natural head movements and eye blinks, but the lip motion is not accurately synchronized with the input voice. Though MakeItTalk [58] can achieve subtle head movements and eye blinks, the mouth shapes are not accurate, which are marked with a box. The lip motion of Wav2lip [34] is accurate, but it can only synthesize the mouth movement of the talking face. AD-NeRF [21] use two NeRFs to generate the head, lower body separately, and we observe a clear white gap between the head part and the body part (marked with a box in the figure). Our method generates photo-realistic talking heads with diverse head movements.

the photo-metric reconstruction error  $\mathcal{L}_{photo}$  between the rendering outputs and the ground truth to train our NeRF:

$$\mathcal{L}_{photo} = \sum_{\mathbf{r} \in \mathcal{R}} \|\hat{C}(\mathbf{r}) - C(\mathbf{r})\|^2, \quad (11)$$

Where  $\mathcal{R}$  means the collections of the rays. Please refer to supplementary material for more information on volume rendering and neural radiance field.

## 4. Experiments

### 4.1. Experimental Setup

**Datasets.** We leverage the LRS2 [10] and HDTF [55] datasets for the face attributes disentanglement and audio to lip synchronization tasks. LRS2 consists of thousands of spoken sentences from BBC television. Each sentence contains up to 100 characters. HDTF is a new dataset with high-resolution videos. It is collected from youtube and consists of about 16 hours of 720P or 1080P videos. In order to compare with previous SOTA methods [21, 30], we also adopt the training videos in AD-Nerf [21] and Live Speech Por-

traits [30]. For the LRS2 and HDTF datasets, we first estimate the 3DMM face expression parameters as in [14] and fix them to the front view. All the video data are resampled to 25 FPS. As for the audio data, we extract the MFCC audio feature with the windows size of 10 milliseconds and make sure that the audio sequences and mouth movements sequences are strictly aligned.

**Evaluation Metrics.** We conduct quantitative evaluations on metrics previously involved in the talking head generation field. We employ Peak Signal-to-Noise Ratio (PSNR) [23] and Structural Similarity (SSIM) [23] to measure the image quality. Besides, we utilize both Landmarks Distance (LMD) [8] around the mouths and the confidence score ( $\text{Sync}_{conf}$ ) proposed in SyncNet [5] to evaluate the accuracy of mouth shapes and lip synchronization. Furthermore, we calculate the eye blink frequency (blinks/s) to evaluate the eye blink naturalness compared to the target person.

### 4.2. Comparison with State-of-the-arts

We compare our DFA-NeRF with the SOTA methods, including three identity-independent approaches, *i.e.*,

Method	Testset A by [30]					Testset B by [30]				
	PSNR $\uparrow$	SSIM $\uparrow$	LMD $\downarrow$	Sync $\uparrow$	blinks/s	PSNR $\uparrow$	SSIM $\uparrow$	LMD $\downarrow$	Sync $\uparrow$	blinks/s
ATVG [9]	26.41	0.803	5.32	7.2	N/A	25.43	0.808	5.63	7.0	N/A
MakeItTalk [58]	26.33	0.814	4.0	7.32	0.37	27.14	0.822	7.62	5.2	0.37
Wav2Lip [34]	27.63	0.854	5.63	<b>9.8</b>	N/A	27.32	0.851	5.45	<b>9.5</b>	N/A
LSP [30]	28.33	0.921	4.72	5.4	0.41	29.36	0.834	4.53	5.2	0.38
AD-NeRF [21]	28.72	0.914	5.42	4.3	0.12	31.12	0.903	4.86	4.5	0.84
Ground Truth	N/A	1.000	0.00	9.4	0.42	N/A	1.000	0.00	7.6	0.32
DFA-NeRF (ours)	<b>29.12</b>	<b>0.938</b>	<b>3.74</b>	7.3	0.46	<b>32.09</b>	<b>0.917</b>	<b>3.84</b>	7.1	0.37

Table 2. Evaluation with different methods. We use the videos *May* and *Obama2* as the testset A and testset B proposed in [30]. We train a new model with the method proposed in AD-NeRF [21] and use the pre-trained models provided by all other methods to compare. We also report the eye blink frequency where N/A means the method fails to generate eye blink motions. Best results are in **bold**.

MOS on / Approach	ATVG	MakeItTalk	Wav2lip	LSP	AD-NeRF	DFA-NeRF (ours)
Auido-Visual Sync	3.42	2.18	3.76	3.66	3.65	<b>3.84</b>
Naturalness of Head Movement	1.32	2.43	1.47	4.03	3.63	<b>4.12</b>
Naturalness of Eye Blink	1.12	3.12	1.32	4.06	2.72	<b>4.08</b>
Realness of Image	1.52	2.24	2.53	<b>3.84</b>	3.63	3.78

Table 3. User study analyses measured by Mean Opinion Scores. Higher is better.

ATVG [9], MakeItTalk [58], Wav2Lip [34] and two identity-specific approaches, *i.e.* AD-NeRF [21] LSP [30].

**Qualitative Results.** As subject evaluation is crucial for talking head generation, we show the generation results compared to the state-of-the-art methods. As Fig. 5 shows, our method can generate more realistic results and diverse head motions. Only our approach and AD-NeRF can generate unlimited resolution videos among these methods. AD-NeRF[21] uses two NeRF to render the head and torso separately and blend them. Therefore, it cannot avoid artifacts appearing at the neck. In contrast, we adopt one NeRF to simultaneously render the head and torso, consequently generating more appealing results.

**Quantitative Results.** The quantitative results are reported in Table 2. It can be observed that our method achieves the best results under most of the metrics on the test dataset. In Testset A, our model achieves 29.12 in PSNR and 0.938 in SSIM, notably outperforming prior arts. Our model also achieves the lowest LMD, which means it can predict the most accurate mouth shapes compared to other methods. As for the experiments on eye blink frequency, we observe that ATVG[9] and Wav2Lip[34] fail to generate the eye blink motions. The eye blink frequency of AD-NeRF[21] is low and the eyes cannot completely close. The eye blink frequency of MakeItTalk[58] is fixed for the two testset. Only our method and LSP[30] can generate personalized eye blinks naturally. The reason for the high Sync<sub>conf</sub> in Wav2Lip [45] is that it only generates the lip movements of

the input videos, and the Sync<sub>conf</sub> is even higher than the ground truth video. The Sync<sub>conf</sub> of our method is closest to the ground truth, which means the input audio and our generated lip motion are well synchronized.

**User Study.** We conduct user studies with 20 attendees on 36 videos generated by ours and the five other methods. The driving audio is selected from three different languages: English, Chinese and German. We adopt the widely used Mean Opinion Scores (MOS) [51] rating protocol. Each participant is asked to rate from 1-5 for the talking-head generation results based on four major aspects: audio-visual synchronization quality, the naturalness of head movement, the naturalness of eye blink and image realness. We collect the rating results and compute the average score of each method. The statistics are shown in Table 3. Most of the method has comparable Audio-Visual synchronized score except for MakeItTalk [58]. Wav2lip [34] and ATVG [9] cannot change head poses and generate eye blink motions. Therefore, their naturalness of head movement and eye blink scores are relatively lower. Although LSP [30] achieves the highest score of the image realness(3.84), our method achieves comparable results(3.78). Users prefer our results on audio-visual synchronization, the naturalness of head movement and eye blink, proving the effectiveness of the proposed method.

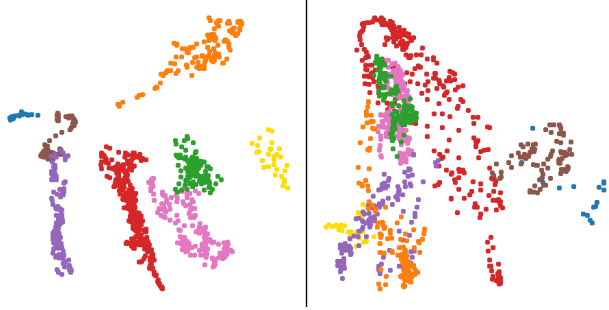


Figure 6. PCA of different people’s personalized face attributes in  $Z$  space. Left: with audio as the condition. Right: without audio as the condition. Different kinds of colors represent different identities. We find that the audio information helps the cross-modal encoder predict personalized face attributes.

Method	D-Rot ↓	D-Pos ↓
MLP VAE	17.81%	20.95%
LSTM VAE	19.06%	22.81%
Trans VAE	3.45%	5.21%
Trans GP-VAE (Ours)	<b>3.19%</b>	<b>4.47%</b>

Table 4. Ablation studies with the structure and sample process of VAE. Trans refers to Transformer.

### 4.3. Further Analysis

**Analysis of Personalized Attributes.** In our framework, we employ audio to predict the personalized attributes. To verify whether the audio information helps identify personal attributes, we visualize the PCA results of different people’s personalized attributes in the  $Z$  space with or without audio. Fig. 6 demonstrates that the personalized attributes are more distinct conditioned on audio.

**Effectiveness of Personalized Attributes.** Here, we analyze the importance of the disentangled eye blink features and synchronized audio features. As shown in Fig. 7, the eyes cannot even close without the eye blink features. Table 5 reveals the impact of different audio features. We use LMD and SyncNet confidence scores to measure the accuracy and synchronization of the lip motion. The results show that MFCC and DeepSpeech[1] features cannot generate synchronized lip motions accurately. With the help of contrastive learning, our feature can generate much better results.

**Impact of VAE Structure and Gaussian Process.** We conduct ablation studies on the structure of VAE and the impact of the Gaussian Process. The results are shown in Table 4. We use D-Rot/Pos in MakeItTalk[58] to measure head rotation and translation prediction accuracy. It can be observed that both MLP and LSTM cannot achieve satisfactory results, where MLP ignores the temporal relation of

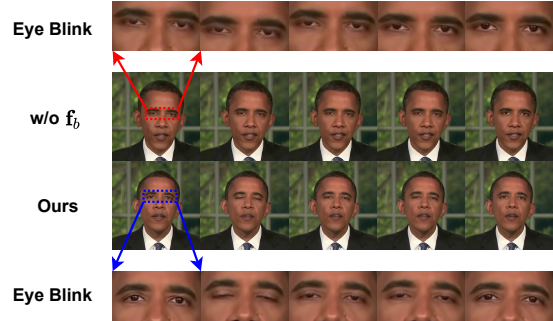


Figure 7. Ablation study of the disentangled eye blink features. We present continuous sequences of synthesized videos. The upper row reveals that the eyes fail to blink without the feature  $f_e$ . Our method can synthesize natural eye blink images with  $f_e$

the time series and LSTM tends to generate still outputs. Transformer-based architecture improves performance significantly, proving the effectiveness of Transformer on long time series prediction. Additionally, Gaussian Process can capture the temporal dynamics among frames, consequently improving the final performance. More analysis and experiments can be found in the supplementary material.

Mehod	LMD ↓	Sync <sub>conf</sub> ↑
MFCC	5.71	4.6
Deep Speech [1]	4.63	5.1
Ground Truth	0.00	7.8
Ours	<b>3.86</b>	<b>7.3</b>

Table 5. Ablation study for the input audio feature in NeRF. We use MFCC features or Deep Speech features as conditions of NeRF. LMD and lip sync scores are adopted to evaluate the lip motion accuracy. Ground Truth refers to the ground truth scores of LMD and Sync<sub>conf</sub>. Our method achieves the best performance.

## 5. Discussion and Conclusion

We have proposed Disentangled Face Attributes NeRF (DFA-NeRF) for talking head generation. We argue that an excellent talking-head video requires three properties, *i.e.*, maintaining lip-syncing at a semantic level, keeping high visual quality and containing personalized spontaneous motions. DFA-NeRF achieves these properties w.r.t. both personalized attributes and lip motion in talking heads with controllable head pose and eye blink. Moreover, quantitative and qualitative experiments demonstrate that our DFA-NeRF can synthesize high-fidelity talking head videos.

**Limitation.** Our method is not applicable for multiple input voices. Studies on speaker diarization splitting up audio into homogeneous segments provide a probable solution. Since we do not focus on fast inference, the rendering



process is time-consuming while this can be relieved by acceleration methods.

**Broader Impacts.** Our method can generate natural and realistic talking head videos with few requirements. So it may bring potential ethical issues and negative social impacts. Therefore, researchers must treat DFA-NeRF cautiously and rationally. Meanwhile, the community should promote studies on face forge detection to automatically keep these videos away from social media

## References

- [1] Dario Amodei, Sundaram Ananthanarayanan, Rishita Anubhai, Jingliang Bai, Eric Battenberg, Carl Case, Jared Casper, Bryan Catanzaro, Qiang Cheng, Guoliang Chen, et al. Deep speech 2: End-to-end speech recognition in english and mandarin. In *ICML*, 2016.
- [2] Robert Anderson, Björn Stenger, Vincent Wan, and Roberto Cipolla. An expressive text-driven 3d talking head. In *SIGGRAPH*, 2013.
- [3] Sarthak Bhagat, Shagun Uppal, Zhuyun Yin, and Nengli Lim. Disentangling multiple features in video sequences using gaussian processes in variational autoencoders. In *ECCV*.
- [4] Chen Cao, Yanlin Weng, Shun Zhou, Yiying Tong, and Kun Zhou. Facewarehouse: A 3d facial expression database for visual computing. *TVCG*, 2014.
- [5] Francesco Paolo Casale, Adrian V. Dalca, Luca Saglietti, Jennifer Listgarten, and Nicoló Fusi. Gaussian process prior variational autoencoders. 2018.
- [6] Lele Chen, Guofeng Cui, Ziyi Kou, Haitian Zheng, and Chenliang Xu. What comprises a good talking-head video generation? 2020.
- [7] Lele Chen, Guofeng Cui, Celong Liu, Zhong Li, Ziyi Kou, Yi Xu, and Chenliang Xu. Talking-head generation with rhythmic head motion. In *ECCV*, 2020.
- [8] Lele Chen, Zhiheng Li, Ross K. Maddox, Zhiyao Duan, and Chenliang Xu. Lip movements generation at a glance. In *ECCV*, 2018.
- [9] Lele Chen, Ross K. Maddox, Zhiyao Duan, and Chenliang Xu. Hierarchical cross-modal talking face generation with dynamic pixel-wise loss. In *CVPR*, 2019.
- [10] Joon Son Chung, Andrew Senior, Oriol Vinyals, and Andrew Zisserman. Lip reading sentences in the wild. In *CVPR*, 2017.
- [11] Joon Son Chung and Andrew Zisserman. Out of time: Automated lip sync in the wild. In *ACCV*, 2016.
- [12] Daniel Cudeiro, Timo Bolkart, Cassidy Laidlaw, Anurag Ranjan, and Michael J. Black. Capture, learning, and synthesis of 3d speaking styles. In *CVPR*, 2019.
- [13] Filipe Antonio de Barros Reis, Paula Dornhofer Paro Costa, and José Mario De Martino. Deeply emotional talking head: A generative adversarial network approach to expressive speech synthesis with emotion control. In *SIGGRAPH Posters*, 2020.
- [14] Yu Deng, Jiaolong Yang, Sicheng Xu, Dong Chen, Yunde Jia, and Xin Tong. Accurate 3d face reconstruction with weakly-supervised learning: From single image to image set. In *CVPRW*, 2019.
- [15] Pif Edwards, Chris Landreth, Eugene Fiume, and Karan Singh. Jali: an animator-centric viseme model for expressive lip synchronization. *TOG*, 2016.
- [16] Bo Fan, Lijuan Wang, Frank K Soong, and Lei Xie. Photo-real talking head with deep bidirectional lstm. In *ICASSP*, 2015.
- [17] Bo Fan, Lei Xie, Shan Yang, Lijuan Wang, and Frank K Soong. A deep bidirectional lstm approach for video-realistic talking head. *Multimedia Tools and Applications*, 2016.
- [18] Vincent Fortuin, Dmitry Baranchuk, Gunnar Rätsch, and Stephan Mandt. GP-VAE: deep probabilistic time series imputation. In *AISTATS*, 2020.
- [19] Guy Gafni, Justus Thies, Michael Zollhofer, and Matthias Nießner. Dynamic neural radiance fields for monocular 4d facial avatar reconstruction. In *CVPR*, 2021.
- [20] Yudong Guo, Jianfei Cai, Boyi Jiang, Jianmin Zheng, et al. Cnn-based real-time dense face reconstruction with inverse-rendered photo-realistic face images. *PAMI*, 2018.
- [21] Yudong Guo, Keyu Chen, Sen Liang, Yong-Jin Liu, Hujun Bao, and Juyong Zhang. Ad-nerf: Audio driven neural radiance fields for talking head synthesis. In *ICCV*, 2021.
- [22] Sepp Hochreiter and Jürgen Schmidhuber. Long short-term memory. *Neural Computation*, 1997.
- [23] Alain Horé and Djemel Ziou. Image quality metrics: PSNR vs. SSIM. In *ICPR*, 2010.
- [24] Tero Karras, Timo Aila, Samuli Laine, Antti Herva, and Jaakko Lehtinen. Audio-driven facial animation by joint end-to-end learning of pose and emotion. *TOG*, 2017.
- [25] Petr Kellnhofer, Lars C Jebe, Andrew Jones, Ryan Spicer, Kari Pulli, and Gordon Wetzstein. Neural lumigraph rendering. In *CVPR*, 2021.
- [26] D. P. Kingma and M. Welling. Auto-encoding variational bayes. In *ICLR*, 2014.
- [27] Prajwal KR, Rudrabha Mukhopadhyay, Jerin Philip, Abhishek Jha, Vinay Namboodiri, and CV Jawahar. Towards automatic face-to-face translation. In *ACMMM*, 2019.
- [28] Avisek Lahiri, Vivek Kwatra, Christian Frueh, John Lewis, and Chris Bregler. Lipsync3d: Data-efficient learning of personalized 3d talking faces from video using pose and lighting normalization. In *CVPR*, 2021.
- [29] Stephen Lombardi, Tomas Simon, Jason M. Saragih, Gabriel Schwartz, Andreas M. Lehrmann, and Yaser Sheikh. Neural volumes: learning dynamic renderable volumes from images. *TOG*, 2019.
- [30] Yuanxun Lu, Jinxiang Chai, and Xun Cao. Live Speech Portraits: Real-time photorealistic talking-head animation. *TOG*, 2021.
- [31] Ben Mildenhall, Pratul P Srinivasan, Matthew Tancik, Jonathan T Barron, Ravi Ramamoorthi, and Ren Ng. Nerf: Representing scenes as neural radiance fields for view synthesis. In *ECCV*, 2020.
- [32] Arsha Nagrani, Samuel Albanie, and Andrew Zisserman. Seeing voices and hearing faces: Cross-modal biometric matching. In *CVPR*, 2018.

- [33] Stylianos Ploumpis, Haoyang Wang, Nick E. Pears, William A. P. Smith, and Stefanos Zafeiriou. Combining 3d morphable models: A large scale face-and-head model. In *CVPR*, 2019.
- [34] KR Prajwal, Rudrabha Mukhopadhyay, Vinay P Namboodiri, and CV Jawahar. A lip sync expert is all you need for speech to lip generation in the wild. In *ACMMM*, 2020.
- [35] Albert Pumarola, Antonio Agudo, Aleix M. Martínez, Alberto Sanfeliu, and Francesc Moreno-Noguer. Ganimation: Anatomically-aware facial animation from a single image. In *ECCV*, 2018.
- [36] Albert Pumarola, Enric Corona, Gerard Pons-Moll, and Francesc Moreno-Noguer. D-nerf: Neural radiance fields for dynamic scenes. In *CVPR*, 2021.
- [37] Kaizhi Qian, Yang Zhang, Shiyu Chang, Xuesong Yang, and Mark Hasegawa-Johnson. Autovc: Zero-shot voice style transfer with only autoencoder loss. In *ICML*, 2019.
- [38] Najmeh Sadoughi and Carlos Busso. Speech-driven expressive talking lips with conditional sequential generative adversarial networks. *IEEE Transactions on Affective Computing*, 2019.
- [39] Oliver Schreer, Roman Englert, Peter Eisert, and Ralf Tanger. Real-time vision and speech driven avatars for multimedia applications. *TMM*, 2008.
- [40] Taiki Shimba, Ryuhei Sakurai, Hirotake Yamazoe, and Joo-Ho Lee. Talking heads synthesis from audio with deep neural networks. In *SI*, 2015.
- [41] Vincent Sitzmann, Michael Zollhöfer, and Gordon Wetzstein. Scene representation networks: Continuous 3d-structure-aware neural scene representations. 2019.
- [42] Yang Song, Jingwen Zhu, Dawei Li, Xiaolong Wang, and Hairong Qi. Talking face generation by conditional recurrent adversarial network. *IJCAI*, 2019.
- [43] Justus Thies, Mohamed Elgharib, Ayush Tewari, Christian Theobalt, and Matthias Nießner. Neural voice puppetry: Audio-driven facial reenactment. In *ECCV*, 2020.
- [44] Ashish Vaswani, Noam Shazeer, Niki Parmar, Jakob Uszkoreit, Llion Jones, Aidan N Gomez, Łukasz Kaiser, and Illia Polosukhin. Attention is all you need. In *NIPS*, 2017.
- [45] Kaisiyuan Wang, Qianyi Wu, Linsen Song, Zhuoqian Yang, Wayne Wu, Chen Qian, Ran He, Yu Qiao, and Chen Change Loy. Mead: A large-scale audio-visual dataset for emotional talking-face generation. In *ECCV*, 2020.
- [46] Lijuan Wang, Wei Han, and Frank K Soong. High quality lip-sync animation for 3d photo-realistic talking head. In *ICASSP*, 2012.
- [47] Lijuan Wang, Xiaojun Qian, Wei Han, and Frank K. Soong. Synthesizing photo-real talking head via trajectory-guided sample selection. In *INTERSPEECH*, 2010.
- [48] Xinsheng Wang, Qicong Xie, Jihua Zhu, Lei Xie, et al. Anyonet: Synchronized speech and talking head generation for arbitrary person. *arXiv preprint arXiv:2108.04325*, 2021.
- [49] Xin Wen, Miao Wang, Christian Richardt, Ze-Yin Chen, and Shi-Min Hu. Photorealistic audio-driven video portraits. *TVCG*, 2020.
- [50] Haozhe Wu, Jia Jia, Haoyu Wang, Yishun Dou, Chao Duan, and Qingshan Deng. Imitating arbitrary talking style for realistic audio-driven talking face synthesis. In *ACMMM*, 2021.
- [51] Jie Xu, Liyuan Xing, Andrew Perkis, and Yuming Jiang. On the properties of mean opinion scores for quality of experience management. In *ISM*, 2011.
- [52] Ran Yi, Zipeng Ye, Juyong Zhang, Hujun Bao, and Yong-Jin Liu. Audio-driven talking face video generation with learning-based personalized head pose. *arXiv preprint arXiv:2002.10137*, 2020.
- [53] Egor Zakharov, Aliaksandra Shysheya, Egor Burkov, and Victor Lempitsky. Few-shot adversarial learning of realistic neural talking head models. In *ICCV*, 2019.
- [54] Chenxu Zhang, Yifan Zhao, Yifei Huang, Ming Zeng, Saifeng Ni, Madhukar Budagavi, and Xiaohu Guo. Facial: Synthesizing dynamic talking face with implicit attribute learning. In *ICCV*, 2021.
- [55] Zhimeng Zhang, Lincheng Li, Yu Ding, and Changjie Fan. Flow-guided one-shot talking face generation with a high-resolution audio-visual dataset. In *CVPR*, 2021.
- [56] Hang Zhou, Yu Liu, Ziwei Liu, Ping Luo, and Xiaogang Wang. Talking face generation by adversarially disentangled audio-visual representation. In *AAAI*, 2019.
- [57] Hang Zhou, Yasheng Sun, Wayne Wu, Chen Change Loy, Xiaogang Wang, and Ziwei Liu. Pose-controllable talking face generation by implicitly modularized audio-visual representation. In *CVPR*, 2021.
- [58] Yang Zhou, Xintong Han, Eli Shechtman, Jose Echevarria, Evangelos Kalogerakis, and Dingzeyu Li. Makelttalk: speaker-aware talking-head animation. *TOG*, 2020.
- [59] Yang Zhou, Zhan Xu, Chris Landreth, Evangelos Kalogerakis, Subhransu Maji, and Karan Singh. Visemenet: Audio-driven animator-centric speech animation. *TOG*, 2018.
- [60] Hao Zhu, Huaibo Huang, Yi Li, Aihua Zheng, and Ran He. Arbitrary talking face generation via attentional audio-visual coherence learning. *IJCAI*, 2020.